Title: Diversity and woodland structure mediate land-surface phenology in Zambia

Authors: Godlee J. L.[1], Ryan C. M.[1], Siampale A.[2], Dexter K. G.[1,3]

[1]School of GeoSciences, University of Edinburgh, Edinburgh, EH9 3FF, United Kingdom

[2]Forestry Department Headquarters - Ministry of Lands and Natural Resources, Cairo Road, Lusaka, Zambia

[3]Royal Botanic Garden Edinburgh, Edinburgh, EH3 5LR, United Kingdom

Corresponding author:

John L. Godlee

johngodlee@gmail.com

School of GeoSciences, University of Edinburgh, Edinburgh, United Kingdom

Acknowledgements

Author contribution statement

JLG conceived the study, conducted the analysis, and wrote the first draft of the manuscript. AS coordinated plot data collection in Zambia, and initial data management. All authors contributed to manuscript revisions.

Data accessibility statement

The data used in this study are held by the Zambian Integrated Land Use Assessment Project (ILUA-II), and were cleaned by the SEOSAW project (Socio-Ecological Observatory for Southern African Woodlands). An anonymised version of the plot data are available at the following DOI: .

Abstract

Land-surface phenology is a key determinant of ecosystem function across the dry tropics, and measures of land-surface phenology are routinely included in earth system models to constrain estimates of productivity. Future variation in phenology can be predicted to some extent from climatic variables, but our understanding of how ecosystem structure mediates variation in phenology is lacking, commonly limited to coarse plant functional types. We combined a dense plot network of 672 sites across deciduous Zambian woodlands with remotely sensed land-surface phenology metrics to investigate the role of tree species diversity, composition, and demographic structure on phenology, including the phenomenon of pre-rain green-up. We found positive effects of tree species diversity on season length and pre-rain green-up, variation among miombo and non-miombo vegetation types in their phenological patterns and biotic drivers of phenology, and a strong effect of large trees as drivers of the pre-rain green-up and senescence lag effects. The study exemplifies the role of biotic diversity as a determinant of ecosystem function, and offers new insights into the factors which determine land-surface phenology across the dry tropics, which can inform earth system modelling approaches.

1 Introduction

The seasonal timing and duration of foliage production (land-surface phenology) is a key mediator of land-atmosphere exchanges. Foliage forms the primary interface between plants, the atmosphere and sunlight (Gu et al., 2003; Penuelas et al., 2009), thus land-surface phenology plays an important role in regulating global carbon, water and nitrogen cycles (Richardson et al., 2013). Carbon-cycling models routinely incorporate land-surface phenological processes, most commonly through remotely-sensed data products (e.g. Bloom et al. 2016), but our understanding of the ecological mechanisms which determine these phenological processes remains under-developed (Whitley et al., 2017). This limits our ability to predict how land-surface phenology will respond to climate and biodiversity change, and how these responses will vary among species and vegetation types (Xia et al., 2015).

At regional scales, land-surface phenology can be predicted using only climatic factors, namely precipitation, diurnal temperature, and light environment (Adole et al., 2018b), but significant local variation exists within biomes in the timing of leaf production which cannot be attributed solely to abiotic environment (Stöckli et al., 2011). It has been repeatedly suggested that the diversity, composition, and demographic structure of plant species plays a role in determining how ecosystems respond to abiotic phenological cues (Adole et al., 2018a; Jeganathan et al., 2014; Fuller, 1999), owing to differences in life history strategy among species and demographic groups, but current implementation of biotic variation in earth system models is often limited to coarse plant functional

types, which are unable to represent the wide variation in phenological patterns observed at local scales (Scheiter et al., 2013; Pavlick et al., 2013).

Across the dry tropics, seasonal oscillations in water availability produce strong cycles of foliage production (Chidumayo, 2001; Dahlin et al., 2016), with knock-on effects for ecosystem function. The phenomenon of pre-rain green-up seen in some tree species within the dry tropics serves as a striking example of adaptation to seasonal variation in water availability (Ryan et al., 2017). Conservative species, i.e. slower growing, with robust leaves and denser wood, may initiate leaf production (green-up) before the wet season has commenced. More acquisitive species and juveniles however, tend to green-up during the wet season creating a dense leaf-flush during the mid-season peak of growth and dropping their leaves earlier as the wet season ends. Both strategies have associated costs and benefits which allow coexistence of species exhibiting a range of phenological syndromes along this spectrum. While conservative species gain a competitive advantage from having fully emerged leaves when the wet season starts, they must also invest heavily in deep root architecture to access dry season groundwater reserves in order to produce foliage during the dry season. Similarly, while acquisitive species minimise the risk of hydraulic failure and mortality by only producing leaves when conditions are amenable, they forfeit growing season length. It has been suggested that variation in phenological strategy among tree species is one mechanism by which increased species diversity increases resilience to drought and maximises productivity in water-limited woodland ecosystems (Stan & Sanchez-Azofeifa, 2019; Morellato et al., 2016). By providing functional redundancy within the ecosystem, leaf production can be maintained under a wider range of conditions, therefore maximising long-term productivity.

In addition to determining productivity, variation in leaf phenology also affects broader ecosystem function. Woodlands with a longer tree growth period support a greater diversity and abundance of wildlife, particularly birds, but also browsing mammals and invertebrates (Cole et al., 2015; Araujo et al., 2017; Morellato et al., 2016; Ogutu et al., 2013). As climate change increases the frequency and severity of drought in water-limited woodlands, it is feared that this will result in severe negative consequences for biodiversity (Bale et al., 2002). The periods of green-up and senescence which bookend the growing season are key times for invertebrate reproduction (Prather et al., 2012) and herbivore browsing activity (Velasque & Del-Claro, 2016; Morellato et al., 2016). Pre-rain green-up provides a valuable source of moisture and nutrients before the wet season, and can moderate the understorey microclimate, increasing humidity, reducing UV exposure, and moderating diurnal oscillations in temperature, reducing ecophysiological stress which can lead to mortality during the dry season. Additionally, a slower rate of green-up caused by tree species greening at different times, i.e. reduced synchronicity, provides an extended period of bud-burst, maintaining the important food source of nutrient rich young leaves for longer. Thus, understanding the determinants of seasonal

patterns of tree leaf production in dry deciduous woodlands can provide valuable information on spatial variation in vulnerability to climate change, and help to model their contribution to earth system models under climate change.

In this study we investigated how tree species diversity, composition, and demographic structure influence three key measurable aspects of the tree phenological cycle of dry tropical woodlands: (1) the lag time between green-up/senescence and the start/end of the wet season, (2) the rates of greening and senescence at the start and end of the seasonal growth phase, and (3) the overall length of the growth period. We hypothesise that: (H_1) sites with greater species diversity will exhibit a longer growth period and greater cumulative green-ness over the course of the growth period, due to a higher resilience to variation in water availability. Additionally, we hypothesise that: (H_2) in sites with greater species diversity the start of the growing season will occur earlier with respect to the onset of rain due to an increased likelihood of containing a species which can green-up early, and that (H_3) due to variation among species in phenological strategy and minimum water requirement, sites with greater tree species diversity will exhibit slower rates of greening and senescence as different species green-up and senesce at different times. We hypothesise that: (H_4) irrespective of species diversity, variation in tree species composition and vegetation type will cause variation in the phenological metrics outlined above. Finally, we hypothesise that: (H_5) sites with larger trees will exhibit earlier pre-rain green-up and later senescence, under the assumption that large trees can better access resilient deep groundwater reserves outside of the wet season.

2 Materials and methods

2.1 Plot data

We used data on tree species diversity and composition across 672 sites from the Zambian Integrated Land Use Assessment Phase II (ILUA-II), conducted in 2014 (Mukosha & Siampale, 2009; Pelletier et al., 2018). Each site consisted of four 20x50 m (0.1 ha) plots positioned in a square around a central point, with a distance of 500 m between each plot (Figure 2). The original census contained 993 sites, which was filtered in order to define study bounds and to ensure data quality. Only sites with $\geq$50 stems ha^{-1} $\geq$10 cm DBH (Diameter at Breast Height) were included in the analysis, to ensure all sites represented woodlands rather than 'grassy savanna', which is considered a separate biome with different species composition and ecosystem processes governing phenology (Parr et al., 2014). Sites dominated by non-native tree species ($\geq$50% of individuals), e.g. *Pinus* spp. and *Eucalyptus* spp. were excluded, as these species may exhibit non-seasonal patterns of foliage production (Broadhead et al., 2003). Of the 56634 trees recorded, 2% were only identified to genus, and 7.7% could not be identified.

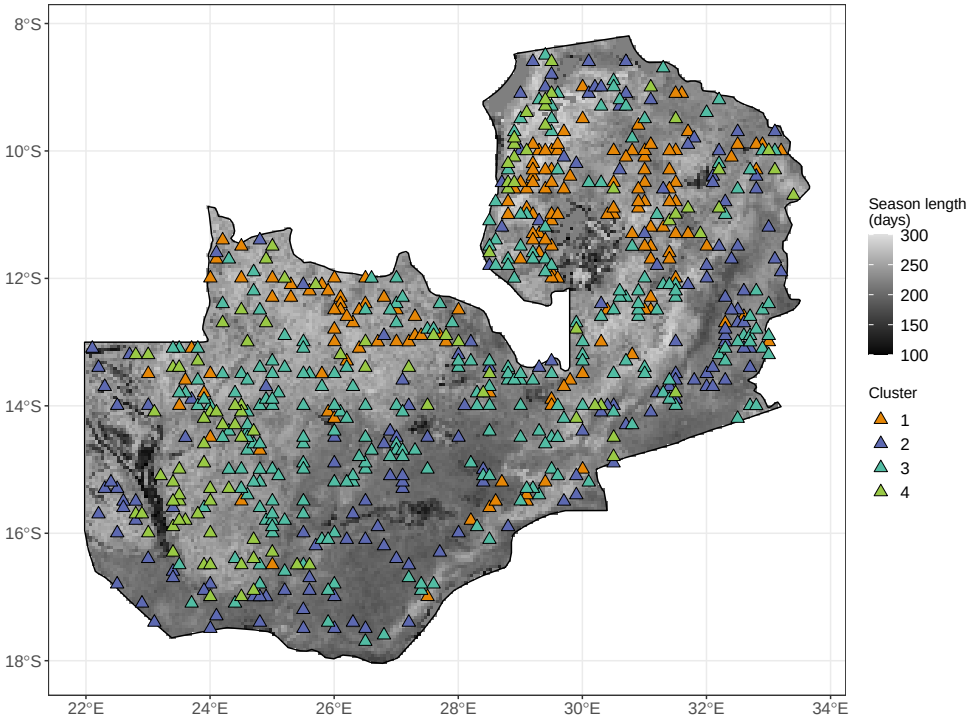

Figure 1: Distribution of study sites within Zambia as triangles, each consisting of four plots. Sites are coloured according to vegetation compositional cluster as identified by Ward's clustering algorithm on the Bray-Curtis distance of plots by species basal area. Zambia is shaded according to growing season length as estimated by the MODIS VIPPHEN-EVI2 product, at 0.05° spatial resolution (Didan & Barreto, 2016).

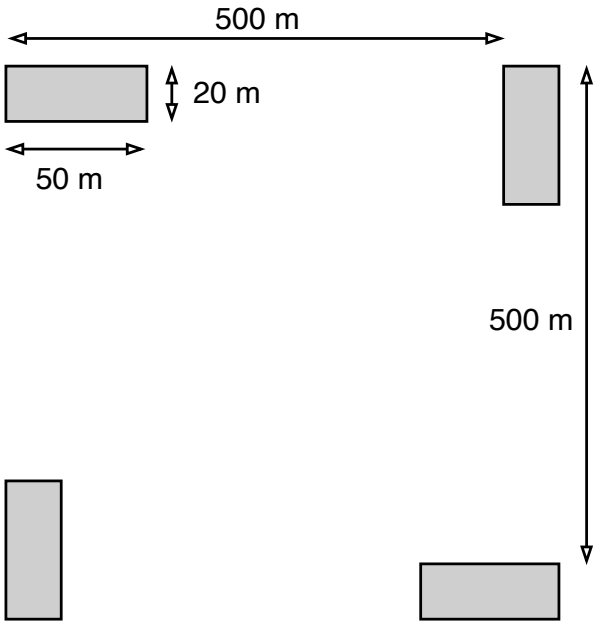

Figure 2: Schematic diagram of plot layout within a site. Each 20x50 m (0.1 ha) plot is shaded grey. Note that the plot dimensions are not to scale.

Within each plot, the species of all trees with at least one stem ≥10 cm DBH were recorded. Plot data was aggregated to the site level for analyses to avoid pseudo-replication caused by the more spatially coarse phenology data. Tree species composition varied little among the four plots within a site, and were treated as representative of the woodland in the local area. Using the Bray-Curtis dissimilarity index on species basal area data (Faith et al., 1987), we calculated that the mean pairwise compositional distance between plots within a site was lower than the mean compositional distance across all pairs of plots in 92% of cases.

2.2 Plot data analysis

To measure variation in tree species composition we used agglomerative hierarchical clustering on species basal area data (Kreft & Jetz, 2010; Fayolle et al., 2014). To guard against sensitivity to rare individuals, which can preclude meaningful cluster delineation across such a large species compositional range, we excluded species with less than five records, and restricted the dataset to sites with more than five species. We used Ward's algorithm to define clusters (Murtagh & Legendre, 2014), based on the Bray-Curtis distance of sites. We determined the optimal number of clusters by maximising the mean silhouette width among clusters (Rousseeuw, 1987). Vegetation type clusters were used later as interaction terms in linear models. We described the vegetation types represented by each of the clusters using a Dufrene-Legendre indicator species analysis (Dufrêne & Legendre, 1997).

To describe the species diversity of each site, we calculated the Shannon-Wiener index (H') from species basal area rather than individual abundance, as a measure of species diversity effectively weighted by a species' contribution to canopy occupancy and thus by contribution to the phenological signal. H' was transformed to the first order numbers-equivalent (^1D) of H', calculated as $e^{H'}$ (Jost, 2007). We use ^1D as the primary measure of species diversity in our statistical models, and is subsequently referred to as species diversity. Additionally, we calculated a separate measure of abundance evenness, using the Shannon Equitability index ($E_{H'}$) (Smith & Wilson, 1996). $E_{H'}$ was calculated as the ratio of basal area Shannon-Wiener diversity index to the natural log of total basal area per site. To describe average tree size, we calculated the quadratic mean of stem diameters per site (Curtis & Marshall, 2000). The quadratic mean gives more weight to large trees and is thus more appropriate for our use, where we are interested in the contribution of large trees to land-surface phenology.

2.3 Land-surface phenology data

To quantify phenology at each site, we used the MODIS MOD13Q1 satellite data product at 250 m resolution (Didan, 2015). The MOD13Q1 product provides an Enhanced Vegetation Index (EVI) time series at 16 day intervals. EVI is widely used as a measure of vegetation growth and is well-correlated with Gross Primary Productivity (GPP), thus providing a measure of land-surface phenology that is relevant to carbon cycling (Sjöström et al., 2011). We used all scenes from January 2010 to December 2020 with less than 20% cloud cover covering the study area. All sites were determined to have a single annual growth season according to the MODIS VIPPHEN product (Didan & Barreto, 2016), which assigns pixels (0.05°, 5.55 km at equator) up to three growth seasons per year. We stacked yearly data between 2010 and 2020 and fit a General Additive Model (GAM) to produce an average EVI curve (Figure 3). We estimated the start and end of the growing season using first derivatives of the GAM. The start of the growing season was identified as the first day where the model slope exceeds half of the maximum positive model slope for a continuous period of 20 or more days, using only backwards looking data, following White et al. (2009). Similarly, we defined the end of the growing season as the final day of the latest 20 period where the GAM slope meets or exceeds half of the maximum negative slope. We estimated the length of the growing season as the number of days between the start and end of the growing season. We calculated cumulative EVI as the EVI accumulated over the growing season, and is reported in the results divided by 100000. We estimated the green-up rate as the slope of a linear model across EVI values between the start of the growing season and the point at which the slope of reduces below half of the maximum positive slope. Similarly the senescence rate was estimated as the slope of a linear model between the latest point where the slope of decrease fell below half of the maximum negative slope

and the end of the growing season. We validated our calculations of cumulative EVI, mean annual EVI, growing season length, season start date, season end date, green-up rate and senescence rate with calculations made by the MODIS VIPPHEN product with linear models comparing the two datasets across our study sites (Figure S1, Table S1). We chose not to use the MODIS VIPPHEN product directly due to its more coarse spatial resolution (0.05°, 5.55 km at equator).

Precipitation data was gathered using the "GPM IMERG Final Precipitation L3 1 day V06" dataset, which has a pixel size of 0.1°(11.1 km at the equator) (Huffman et al., 2015), between 2010 and 2020. Daily total precipitation was separated into three periods: precipitation during the growing season (wet season precipitation), precipitation in the 90 day period before the onset of the growing season (pre-green-up precipitation), and precipitation in 90 day period before the onset of senescence at the end of the growing season (pre-senescence precipitation). Wet season limits were defined as for the EVI data, using the first derivative of a GAM to create a curve for each site using stacked yearly precipitation data, from which we estimated the half-maximum positive and negative slope to identify where the GAM model exceeded these slope thresholds for a consistent period of 20 days or more. Mean diurnal temperature range (Diurnal δT) was calculated as the mean of monthly temperature range from the WorldClim database, using the BioClim variables, with a pixel size of 30 arc seconds (926 m at the equator) (Fick & Hijmans, 2017), averaged across all years of available data (1970-2000). We calculated the lag between the onset of the growing season and the onset of the wet season as the difference between these two dates as calculated above. We performed a similar calculation to estimate the lag between the end of the growing season and the end of the wet season.

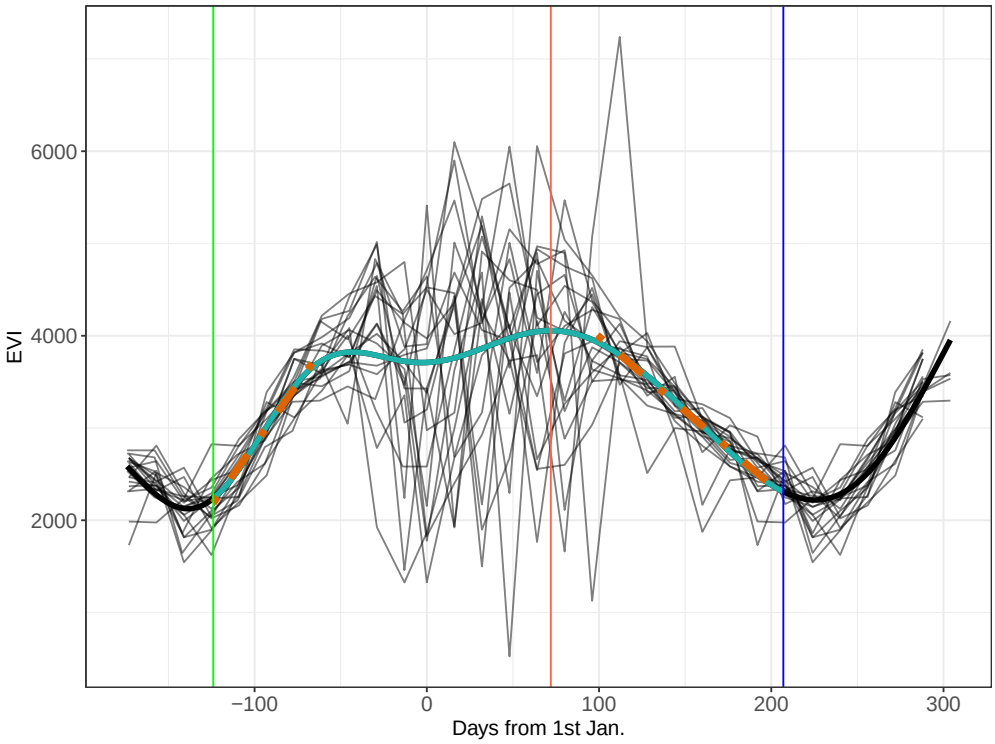

Figure 3: Example EVI time series, demonstrating the metrics derived from it. Thin black lines show the raw EVI time series, with one line for each annual growth season. The thick black line shows the GAM fit. The thin blue lines show the minima which bound the growing season. The red line shows the maximum EVI value reached within the growing season. The shaded cyan area of the GAM fit shows the growing season, as defined by the first derivative of the GAM curve. The two orange dashed lines are linear regressions predicting the green-up rate and senescence rate at the start and end of the growing season, respectively. Note that while the raw EVI time series fluctuate greatly around the middle of the growing season, mostly due to cloud cover, the GAM fit effectively smooths this variation to estimate the average EVI during the mid-season period.

2.3.1 Statistical modelling

We used linear mixed effects models to assess the role of tree species diversity on each phenological metric. We defined a maximal model structure including the fixed effects of species diversity and evenness, alongside climatic variables shown by previous studies to strongly influence land-surface phenology, with vegetation cluster as a random slope effect on species diversity. The maximal model was compared to models with different subsets of fixed effects using the model log likelihood, AIC (Akaike Information Criteria), BIC (Bayesian Information Criteria), and adjusted R^2 values for each model, to determine which combination of fixed effects best explained each phenological metric. Where two similar models were within 2 AIC points of each other, the model with fewer terms was chosen as the best model, to maximise model parsimony. All models were fitted using Maximum

Likelihood (ML) to allow comparison of models with different fixed effects (Zuur et al., 2009). The best model was subsequently re-fitted using Restricted Maximum Likelihood (REML) for model effect size estimation. Fixed effects in each model were transformed to achieve normality where necessary and standardised to Z-scores prior to modelling to allow comparison of slope coefficients within a given model.

We used the `ggeffects` package to estimate the marginal means of the effect of species diversity on each phenological metric among vegetation clusters (Lüdecke, 2018). Estimating marginal means entails generating model predictions across values of a focal variable, in this case species diversity, while holding non-focal variables constant at their reference value. All statistical analyses were conducted in R version 4.0.2 (R Core Team, 2020).

To investigate the effect of tree size on each phenological metric, we conducted a separate set of linear mixed effects models, including the fixed effect of tree size and vegetation cluster as a random intercept term. We used fixed effect sizes to determine the effect of tree size on each phenological metric.

To describe variation within and among vegetation clusters in their land-surface phenology we conducted a simple MANOVA using the phenological metrics as response variables, followed by post-hoc Tukey's tests between each pairwise combination of vegetation clusters per phenological metric, to test whether vegetation clusters differed significantly in their land-surface phenology.

3 Results

Model selection showed that both diversity and evenness were significant fixed effects in models predicting cumulative EVI, season length, and green-up lag (Figure 4), while senescence rate, senescence lag, and green-up rate were poorly predicted across all our models (Table 2). As expected (H_1), species diversity and wet season precipitation both had positive significant effects on cumulative EVI and season length. In contrast, abundance evenness, the other aspect of tree species diversity in our models, had a significant negative effect on both cumulative EVI and season length (Figure 4).

Species diversity caused a significant increase in the green-up lag, i.e. the length of the period between green-up and wet season onset (H_2). This effect was comparable to the effects of pre-green-up precipitation and diurnal temperature range, which also caused an increase in green-up lag (Table 2). The best model predicting green-up lag explained 34% of the variance in this phenological metric. In contrast, senescence lag was poorly defined by our models. The effects of diurnal temperature range and wet season precipitation had wide confidence intervals in the best model for senescence lag, and explained only 8% of the variance in senescence lag. Green-up and senescence rates (H_3) were also poorly constrained in our models, with neither of the best models being appreciably better

than a climate only model according to AIC (Table 2), and only explaining 18% and 15% of the variance in these phenological metrics, respectively.

Four vegetation type clusters were identified during hierarchical clustering. The silhouette value of the clustering algorithm reached 0.59. Cluster 2, consists of small stature Zambesian woodlands, as referenced by Dinerstein et al. (2017) and Chidumayo (2001), and is not dominated by a particular large canopy tree species. It is possible that these woodlands represent highly disturbed miombo woodlands where large trees may have been removed by humans, or alternatively represent resource-limited woodlands due to their low precipitation. Clusters 1, 3 and 4 represent varieties of miombo woodland, dominated by *Brachystegia* spp. and *Julbernardia* spp., with different secondary species. Median species richness is similar across vegetation clusters (Table 1).

The slope of the relationship between species diversity and phenological metrics varied among vegetation clusters (H_4) (Figure 5). According to post-hoc Tukey's tests on marginal effects, Cluster 2 differed from all other clusters in the effect of species diversity on cumulative EVI and season length, and differed from Cluster 1 in the effect of species diversity on green-up lag. The effect of species diversity on green-up lag remained strongly similarly positive across all vegetation clusters. The effect of species diversity in Clusters 1, 3 and 4 did not differ significantly for any other phenological metric (Table S8).

Clusters, 1, 3 and 4 were largely similar in their density distribution of the six phenological metrics, while Cluster 2 had more plots with lower cumulative EVI and lower season length Figure 7. A MANOVA including all phenological metrics showed a significant difference among vegetation clusters ($F(3,668)=14.5$, $p<0.01$). Post-hoc Tukey's tests showed significant differences between Cluster 2 and the other three clusters for all phenological metrics (Table S9). There was little spatial structure to the vegetation clusters identified (Figure 1). The key emergent trends were that Cluster 1 was largely absent from the southwest of the country. Cluster 4 dominated the southwest of the country, possibly representing drier Angolan miombo woodland.

Average tree size, measured by the quadratic mean of stem DBH, caused a greater degree of pre-rain green-up, and also increased the growing season beyond the end of the wet season (H_5, Figure 6). None of the other phenological metrics were significantly affected by average tree size.

Cluster	N sites	Richness	MAP	δT	Species	Indicator value
					Brachystegia longifolia	0.397
1	158	16(8)	1173(158.6)	13(1.5)	*Uapaca kirkiana*	0.390
					Marquesia macroura	0.285
					Combretum molle	0.258
2	158	13(6)	946(173.8)	14(1.6)	*Lannea discolor*	0.228
					Combretum zeyheri	0.214
					Julbernardia paniculata	0.559
3	257	16(7)	999(160.6)	14(1.5)	*Brachystegia boehmii*	0.540
					Pseudolachnostylis maprouneifolia	0.226
					Brachystegia spiciformis	0.582
4	99	14(6)	1011(183.5)	14(1.7)	*Cryptosepalum exfoliatum*	0.285
					Guibourtia coleosperma	0.281

Table 1: Climatic information and Dufrene-Legendre indicator species analysis for the vegetation type clusters identified by the PAM algorithm, based on basal area weighted species abundances. The three species per cluster with the highest indicator values are shown along with other key statistics for each cluster. MAP (Mean Annual Precipitation) and δT (Diurnal temperature range) are reported as the mean and 1 standard deviation in parentheses. Species richness is reported as the median and the interquartile range in parentheses.

Response	δAIC	δBIC	R^2_{adj}	δlogLik
Cumulative EVI	7.2	-1.8	0.31	-5.60
Season length	2.1	-6.9	0.16	-3.07
Green-up rate	-3.2	-12.3	0.18	-0.38
Senescence rate	1.5	-7.5	0.15	-2.77
Green-up lag	20.4	11.4	0.34	-12.19
Senescence lag	-3.6	-12.6	0.08	-0.19

Table 2: Model fit statistics for the best model describing each phenological metric.

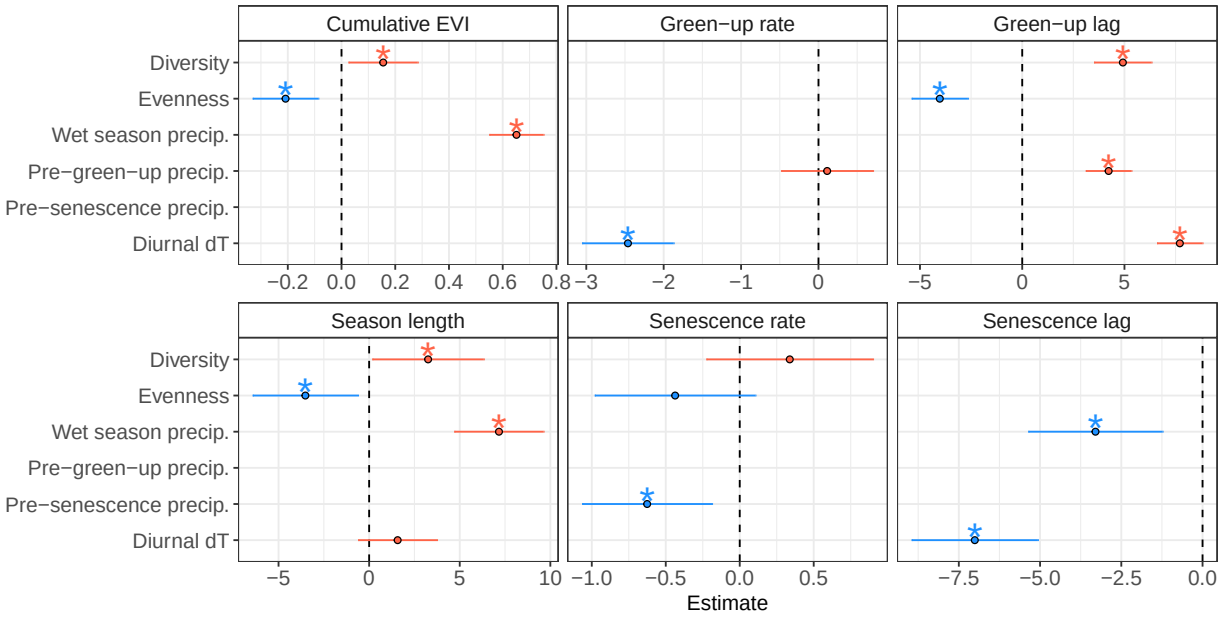

Figure 4: Standardized slope coefficients for each best model of a phenological metric. Slope estimates are ±1 standard error. Slope estimates where the interval does not overlap zero are considered to be significant effects and are marked by asterisks.

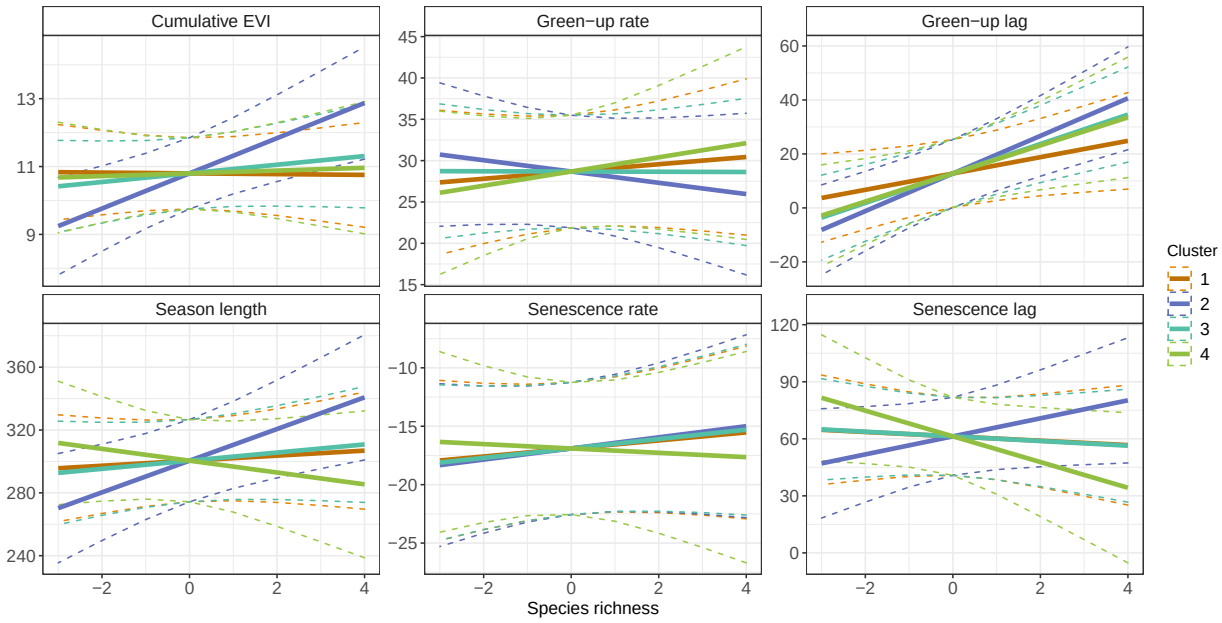

Figure 5: Marginal effects of tree species diversity on each of the phenological metrics, using the maximal mixed effects model, for each vegetation cluster. Dotted lines represent 95% confidence intervals.

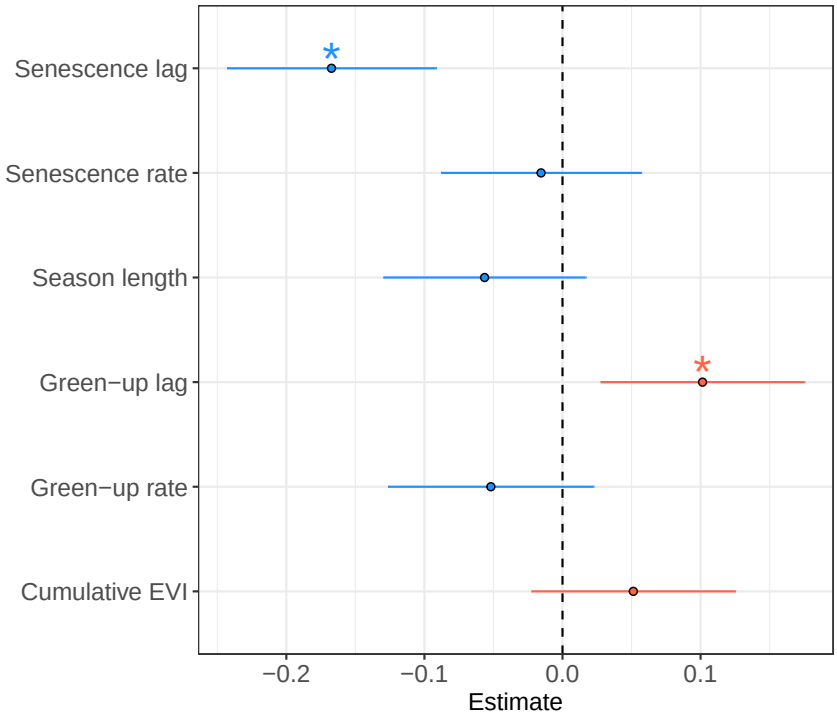

Figure 6: Standardized slope coefficients for the fixed effect of average tree size on each phenological metric. Slope estimates are ±1 standard error. Slope estimates where the interval does not overlap zero are considered to be significant effects and are marked by asterisks.

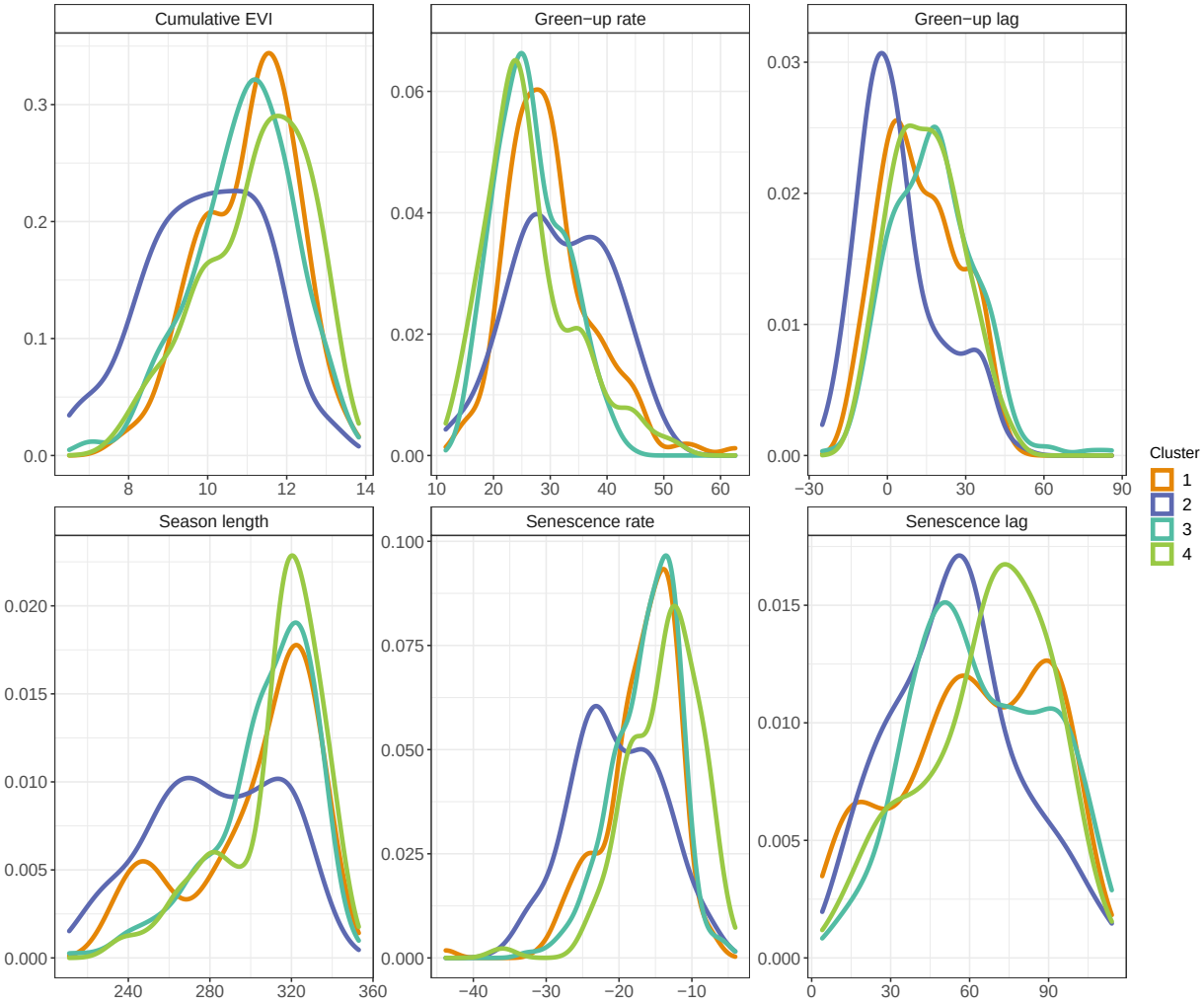

Figure 7: Density distribution of the six phenological metrics used in the study, grouped by vegetation cluster.

4 Discussion

In this study we have demonstrated clear and measurable effects of tree species diversity, species composition, and woodland structure on various aspects of land-surface phenology in Zambian deciduous savannas. We showed that tree species diversity led to an increase in cumulative EVI and season length. Additionally, species diversity caused the onset of greening to occur earlier with respect to the start of the wet season. We also showed that woodlands comprising larger trees are able to maintain a longer growing season by allowing earlier pre-rain green-up, and by extending the end of the growing season. Our study lends support for a positive biodiversity - ecosystem function relationship in deciduous savannas, operating through its influence on phenology. Our results exemplify the role of tree species diversity as a driver of key ecosystem processes, which affect ecosystem structure, the wildlife provisioning role, and gross primary productivity.

Our finding that species diversity strongly affects patterns of land-surface phenology in deciduous Zambian woodlands provides earth surface system modellers with a means to better understand how future changes in species diversity and composition will affect land-surface phenology and therefore the carbon cycle. Incorporating predictions of biotic change into carbon cycling models has been slow, owing to large uncertainties in the effects of diversity on Gross Primary Productivity (GPP). Our study provides a link by demonstrating a strong positive relationship between species diversity and EVI, which itself drives GPP.

Patterns of senescence were poorly predicted by species diversity and evenness in our models. Cho et al. (2017) found that tree cover, measured by MODIS LAI data, had a significant effect on senescence rates in savannas in South Africa, which have similar climatic conditions to the sites in our study. In sparse savannas, while the onset of the growing season is often driven by tree photosynthetic activity, which may precede the onset of precipitation, the end of the growing season is conversely driven by the understorey grass layer, which can itself be dependent on tree cover (Cho et al., 2017; Guan et al., 2014). Grass activity is much more reactive to short-term changes in soil moisture than tree activity, and may oscillate within the senescence period. This may explain the lack of a strong precipitation signal for senescence lag and senescence rate in our models.

Other studies both globally and within southern African savannas have largely ignored patterns of senescence, instead focussing patterns of green-up (Gallinat et al., 2015). Most commonly, these studies simply correlate the decline of rainfall with senescence, but our best model suggests that diurnal temperature range is a stronger determinant of the end of the growing season than precipitation. Alternatively, Zani et al. (2020) suggests that in resource limited environments, senescence times may largely be set by the preceding photosynthetic activity and sink-limitations on growth. For example, limited nutrient supply may prohibit photosynthesis late in the season if the preceding photosynthetic activity has depleted that supply. Reich et al. (1992) suggested that there may be direct constraints on leaf life-span, especially in disturbance and drought-prone environments such as those studied here, which would lead to senescence rate being set largely by the time since bud-burst. Our study corroborates this theory, showing that precipitation across the entire wet season was a better predictor of senescence lag than pre-senescence precipitation, while pre-senescence precipitation does cause variation in the rate of senescence.

While leaf senescence may not be as important for the survival of browsing herbivores as the green-up period, the timing of senescence with respect to temperature and precipitation has important consequences for the savanna understorey microclimate. The longer leaf material remains in the canopy after the end of the wet season, the greater the microclimatic buffer for herbaceous understorey plants and animals, which require water and protection from high levels of insolation and dry air which can prevail rapidly after the end of the wet season (Guan et al., 2014). Our study merely

exemplifies that more work needs to be done to properly characterise the drivers of senescence in this biome, which were poorly constrained in our models.

While species diversity is a common measure of biodiversity, abundance evenness constitutes a second key but related axis (Wilsey et al., 2005; Hillebrand et al., 2008; Jost, 2010). In this study, we found contrasting effects of diversity and evenness on cumulative EVI, season length and green-up lag. Evenness caused a decrease in these phenological metrics, which we did not expect. It is possible that the negative effect of abundance evenness occurred because an increase in evenness is associated with a reduction in the dominance of a few large canopy miombo tree species (e.g. *Brachystegia boehmii* and *Julbernardia paniculata*), as part of the transition from woody savanna to the thicket vegetation represented by vegetation Cluster 2. Large canopy tree species have access to groundwater for a longer part of the year, due to their deep root systems and conservative growth patterns. Indeed, our study found that plots with larger trees tend to green-up earlier and senesce later with respect to the start and end of the wet season. The effect of species diversity on cumulative EVI and season length was driven largely by the response of vegetation Cluster 2, which consisted of shorter stature non-miombo vegetation, while Clusters 1, 3 and 4, which consisted of miombo vegetation, exhibited negligible species diversity effects on these two phenological metrics. In miombo vegetation, it appears that dominant canopy forming tree species drive productivity through selection effects, while in the resource-limited scrubby vegetation represented by Cluster 2, a genuine species diversity effect driven by niche complementarity exists.

Our coverage of very short growing season lengths in Zambia was restricted, with a notable absence of plot data in the northeast of the country around 30.5°E, 11.5°S, and 23.0°E, 15.0°S. Upon further inspection of true colour satellite imagery, these regions are largely seasonally water-logged floodplain and swampland, and were likely ignored by the ILUA-II assessment for this reason. This also explains their divergent phenological patterns as observed in the MODIS EVI data. While our study focusses on woodlands, the phenological behaviour of these other vegetation types should also be considered in future studies, as these may be even more sensitive to changes in climate (Dean et al., 2018) and under greater land-use change pressures (Langan et al., 2018).

It is important to note that the remotely sensed EVI measurements used here aren't specific only to trees, they represent the landscape as a singe unit. Nevertheless, seasonal patterns of tree leaf phenology in southern African deciduous woodlands, particularly the pre-rain green-up phenomenon, is driven almost exclusively by trees, while grasses tend to follow patterns of precipitation more closely (Whitecross et al., 2017; Archibald & Scholes, 2007; Higgins et al., 2011). Grasses contribute to gross primary productivity, and it was therefore in our interests to include their response in our analysis as we seek to demonstrate how tree species diversity can affect cycles of carbon exchange. Additionally, the micro-climatic effects of tree leaf canopy coverage and hydraulic lift through tree

deep root systems will benefit the productivity of grasses as well as understorey tree individuals.

5 Conclusion

Here we explored the role of tree species diversity, composition and woodland structure on land surface phenology across Zambia. We showed that species diversity clearly affects the lag time between wet season onset and growth, the length of the growing season, and ultimately woodland productivity, as measured by cumulative EVI. We also demonstrated the effect of woodland demographic structure on land surface phenology, with woodlands consisting of larger trees maintaining a longer growing season, extending it beyond the wet season. Finally, we have demonstrated variation in phenological patterns among vegetation types within Zambia that are commonly not distinguished between in earth system models. Our results have a range of consequences for earth system modellers as well as conservation managers working in Zambia and across the dry tropics, and lend further support to an already well established corpus of the positive effect of species diversity on ecosystem function.

References

Adole, T., J. Dash & P. M. Atkinson (2018a). "Characterising the land surface phenology of Africa using 500 m MODIS EVI". In: *Applied Geography* 90, pp. 187–199. DOI: 10.1016/j.apgeog.2017.12.006.

Adole, T., J. Dash & P. M. Atkinson (2018b). "Large-scale prerain vegetation green-up across Africa". In: *Global Change Biology* 24.9, pp. 4054–4068. DOI: 10.1111/gcb.14310.

Araujo, H. F. P. de, A. H. Vieira-Filho, M. R. V. Barbosa, J. A. F. Diniz-Filho & J. M. C. da Silva (2017). "Passerine phenology in the largest tropical dry forest of South America: Effects of climate and resource availability". In: *Emu - Austral Ornithology* 117.1, pp. 78–91. DOI: 10.1080/01584197.2016.1265430.

Archibald, S. & R. J. Scholes (2007). "Leaf green-up in a semi-arid African savanna -separating tree and grass responses to environmental cues". In: *Journal of Vegetation Science* 18.4, pp. 583–594. DOI: 10.1111/j.1654-1103.2007.tb02572.x.

Bale, J. S., G. J. Masters, I. D. Hodkinson, C. Awmack, T. M. Bezemer, V. K. Brown, J. Butterfield, A. Buse, J. C. Coulson, J. Farrar, et al. (2002). "Herbivory in global climate change research: direct effects of rising temperature on insect herbivores". In: *Global Change Biology* 8.1, pp. 1–16. DOI: 10.1046/j.1365-2486.2002.00451.x.

Bloom, A. A., J. Exbrayat, I. R. van der Velde, L. Feng & M. Williams (2016). "The decadal state of the terrestrial carbon cycle: Global retrievals of terrestrial carbon allocation, pools, and

residence times". In: *Proceedings of the National Academy of Sciences* 113.5, pp. 1285–1290. DOI: 10.1073/pnas.1515160113.

Broadhead, J. S., C. K. Ong & C. R. Black (2003). "Tree phenology and water availability in semi-arid agroforestry systems". In: *Forest Ecology and Management* 180.1-3, pp. 61–73. DOI: 10.1016/s0378-1127(02)00602-3.

Chidumayo, E. N. (2001). "Climate and phenology of savanna vegetation in southern Africa". In: *Journal of Vegetation Science* 12.3, p. 347. DOI: 10.2307/3236848.

Cho, M. A., A. Ramoelo & L. Dziba (2017). "Response of land surface phenology to variation in tree cover during green-up and senescence periods in the semi-arid savanna of southern Africa". In: *Remote Sensing* 9.7, p. 689. DOI: 10.3390/rs9070689.

Cole, E. F., P. R. Long, P. Zelazowski, M. Szulkin & B. C. Sheldon (2015). "Predicting bird phenology from space: Satellite-derived vegetation green-up signal uncovers spatial variation in phenological synchrony between birds and their environment". In: *Ecology and Evolution* 5.21, pp. 5057–5074. DOI: 10.1002/ece3.1745.

Curtis, R. O. & D. D. Marshall (2000). "Technical Note: Why Quadratic Mean Diameter?" In: 15.3, pp. 137–139. DOI: 10.1093/wjaf/15.3.137.

Dahlin, K. M., D. Del Ponte, E. Setlock & R. Nagelkirk (2016). "Global patterns of drought deciduous phenology in semi-arid and savanna-type ecosystems". In: *Ecography* 40.2, pp. 314–323. DOI: 10.1111/ecog.02443.

Dean, J. F., J. J. Middelburg, T. Röckmann, R. Aerts, L. G. Blauw, M. Egger, M. S. M. Jetten, A. E. E. de Jong, O. H. Meisel, O. Rasigraf, et al. (2018). "Methane Feedbacks to the Global Climate System in a Warmer World". In: *Reviews of Geophysics* 56.1, pp. 207–250. DOI: 10.1002/2017rg000559.

Didan, L. (2015). *MOD13Q1 MODIS/Terra Vegetation Indices 16-Day L3 Global 250m SIN Grid V006 [Data set]*. NASA EOSDIS Land Processes DAAC. DOI: 10.5067/MODIS/MOD13Q1.006. (Visited on 08/05/2020).

Didan, L. & A. Barreto (2016). *NASA MEaSUREs Vegetation Index and Phenology (VIP) Phenology EVI2 Yearly Global 0.05Deg CMG [Data set]*. NASA EOSDIS Land Processes DAAC. DOI: 10.5067/MEaSUREs/VIP/VIPPHEN_EVI2.004. (Visited on 08/05/2020).

Dinerstein, E., D. Olson, A. Joshi, C. Vynne, N. D. Burgess, E. Wikramanayake, N. Hahn, S. Palminteri, P. Hedao, R. Noss, et al. (2017). "An ecoregion-based approach to protecting half the terrestrial realm". In: *BioScience* 67.6, pp. 534–545. DOI: 10.1093/biosci/bix014.

Dufrêne, M. & P. Legendre (1997). "Species assemblage and indicator species: The need for a flexible asymmetrical approach". In: *Ecological Monographs* 67, pp. 345–366. DOI: 10.1890/0012-9615(1997)067[0345:SAAIST]2.0.CO;2.

Faith, D. P., P. R. Minchin & L. Belbin (Apr. 1987). "Compositional dissimilarity as a robust measure of ecological distance". In: *Vegetatio* 69.1-3, pp. 57–68. DOI: 10.1007/bf00038687. URL: https://doi.org/10.1007/bf00038687.

Fayolle, A., M. D. Swaine, J. Bastin, N. Bourland, J. A. Comiskey, G. Dauby, J. Doucet, J. Gillet, S. Gourlet-Fleury, O. J. Hardy, et al. (2014). "Patterns of tree species composition across tropical African forests". In: *Journal of Biogeography* 41.12, pp. 2320–2331. DOI: 10.1111/jbi.12382.

Fick, S. E. & R. J. Hijmans (2017). "WorldClim 2: New 1-km spatial resolution climate surfaces for global land areas". In: *International Journal of Climatology* 37.12, pp. 4302–4315. DOI: 10.1002/joc.5086.

Fuller, D. O. (1999). "Canopy phenology of some mopane and miombo woodlands in eastern Zambia". In: *Global Ecology and Biogeography* 8.3-4, pp. 199–209. DOI: 10.1046/j.1365-2699.1999.00130.x.

Gallinat, A. S., R. B. Primack & D. L. Wagner (2015). "Autumn, the neglected season in climate change research". In: 30.3, pp. 169–176. DOI: 10.1016/j.tree.2015.01.004.

Gu, L., W. M. Post, D. Baldocchi, T. A. Black, S. B. Verma, T. Vesala & S. C. Wofsy (2003). "Phenology of vegetation photosynthesis". In: *Phenology: An Integrative Environmental Science*. Springer Netherlands, pp. 467–485. DOI: 10.1007/978-94-007-0632-3_29.

Guan, K., E. F. Wood, D. Medvigy, J. Kimball, M. Pan, K. K. Caylor, J. Sheffield, C. Xu & M. O. Jones (2014). "Terrestrial hydrological controls on land surface phenology of African savannas and woodlands". In: *Journal of Geophysical Research: Biogeosciences* 119.8, pp. 1652–1669. DOI: 10.1002/2013jg002572.

Higgins, S. I., M. D. Delgado-Cartay, E. C. February & H. J. Combrink (2011). "Is there a temporal niche separation in the leaf phenology of savanna trees and grasses?" In: *Journal of Biogeography* 38.11, pp. 2165–2175. DOI: 10.1111/j.1365-2699.2011.02549.x.

Hillebrand, H., D. M. Bennett & M. W. Cadotte (2008). "Consequences of dominance: A review of evenness effects on local and regional ecosystem processes". In: *Ecology* 89.6, pp. 1510–1520. DOI: 10.1890/07-1053.1.

Huffman, G. J., E. F. Stocker, D. Bolvin, E. J. Nelkin & J. Tan (2015). *GPM IMERG Final Precipitation L3 1 day 0.1 degree x 0.1 degree V06 [Data set]*. Goddard Earth Sciences Data and Information Services Center (GES DISC). DOI: 10.5067/MODIS/MOD13Q1.006. (Visited on 10/30/2020).

Jeganathan, C., J. Dash & P. M. Atkinson (2014). "Remotely sensed trends in the phenology of northern high latitude terrestrial vegetation, controlling for land cover change and vegetation type". In: *Remote Sensing of Environment* 143, pp. 154–170. DOI: 10.1016/j.rse.2013.11.020.

Jost, L. (2007). "Partitioning diversity into independent alpha and beta components". In: *Ecology* 88.10, pp. 2427–2439. DOI: 10.1890/06-1736.1.

Jost, L. (2010). "The relation between evenness and diversity". In: *Diversity* 2.2, pp. 207–232. DOI: 10.3390/d2020207.

Kreft, H. & W. Jetz (2010). "A framework for delineating biogeographical regions based on species distributions". In: *Journal of Biogeography* 37.11, pp. 2029–2053. DOI: 10.1111/j.1365-2699.2010.02375.x.

Langan, C., J. Farmer, M. Rivington & J. U. Smith (2018). "Tropical wetland ecosystem service assessments in East Africa: A review of approaches and challenges". In: 102, pp. 260–273. DOI: 10.1016/j.envsoft.2018.01.022.

Lüdecke, D. (2018). "ggeffects: Tidy data frames of marginal effects from regression models." In: *Journal of Open Source Software* 3.26, p. 772. DOI: 10.21105/joss.00772.

Morellato, L. P. C., B. Alberton, S. T. Alvarado, B. Borges, E. Buisson, M. G. G. Camargo, L. F. Cancian, D. W. Carstensen, D. F. E. Escobar, P. T. P. Leite, et al. (2016). "Linking plant phenology to conservation biology". In: *Biological Conservation* 195, pp. 60–72. DOI: 10.1016/j.biocon.2015.12.033.

Mukosha, J. & A. Siampale (2009). *Integrated land use assessment Zambia 2005–2008*. Lusaka, Zambia: Ministry of Tourism, Environment et al.

Murtagh, F. & P. Legendre (2014). "Ward's hierarchical agglomerative clustering nethod: Which algorithms implement Ward's criterion?" In: *Journal of Classification* 31.3, pp. 274–295. DOI: 10.1007/s00357-014-9161-z.

Ogutu, J. O., H. Piepho & H. T. Dublin (2013). "Responses of phenology, synchrony and fecundity of breeding by African ungulates to interannual variation in rainfall". In: *Wildlife Research* 40.8, p. 698. DOI: 10.1071/wr13117.

Parr, C. L., C. E. R. Lehmann, W. J. Bond, W. A. Hoffmann & A. N. Andersen (2014). "Tropical grassy biomes: Misunderstood, neglected, and under threat". In: *Trends in Ecology and Evolution* 29, pp. 205–213. DOI: 10.1016/j.tree.2014.02.004.

Pavlick, R., D. T. Drewry, K. Bohn, B. Reu & A. Kleidon (2013). "The Jena Diversity-Dynamic Global Vegetation Model (JeDi-DGVM): A diverse approach to representing terrestrial biogeography and biogeochemistry based on plant functional trade-offs". In: *Biogeosciences* 10.6, pp. 4137–4177. DOI: 10.5194/bg-10-4137-2013.

Pelletier, J., A. Paquette, K. Mbindo, N. Zimba, A. Siampale, B. Chendauka, F. Siangulube & J. W. Roberts (2018). "Carbon sink despite large deforestation in African tropical dry forests (miombo woodlands)". In: *Environmental Research Letters* 13, p. 094017. DOI: 10.1088/1748-9326/aadc9a.

Penuelas, J., T. Rutishauser & I. Filella (2009). "Phenology feedbacks on climate change". In: *Science* 324.5929, pp. 887–888. DOI: 10.1126/science.1173004.

Prather, C. M., S. L. Pelini, A. Laws, E. Rivest, M. Woltz, C. P. Bloch, I. Del Toro, C. Ho, J. Kominoski, T. A. S. Newbold, et al. (2012). "Invertebrates, ecosystem services and climate change". In: *Biological Reviews* 88.2, pp. 327–348. DOI: 10.1111/brv.12002.

R Core Team (2020). *R: A Language and Environment for Statistical Computing*. R Foundation for Statistical Computing. Vienna, Austria. URL: https://www.R-project.org/.

Reich, P. B., M. B. Walters & D. S. Ellsworth (1992). "Leaf life-span in relation to leaf, plant, and stand characteristics among diverse ecosystems". In: 62.3, pp. 365–392. DOI: 10.2307/2937116.

Richardson, A. D., T. F. Keenan, M. Migliavacca, Y. Ryu, O. Sonnentag & M. Toomey (2013). "Climate change, phenology, and phenological control of vegetation feedbacks to the climate system". In: *Agricultural and Forest Meteorology* 169, pp. 156–173. DOI: 10.1016/j.agrformet.2012.09.012.

Rousseeuw, P. J. (1987). "Silhouettes: A graphical aid to the interpretation and validation of cluster analysis". In: *Journal of Computational and Applied Mathematics* 20, pp. 53–65. DOI: 10.1016/0377-0427(87)90125-7.

Ryan, C. M., M. Williams, J. Grace, E. Woollen & C. E. R. Lehmann (2017). "Pre-rain green-up is ubiquitous across southern tropical Africa: implications for temporal niche separation and model representation". In: *New Phytologist* 213.2, pp. 625–633. DOI: 10.1111/nph.14262.

Scheiter, S., L. Langan & S. I. Higgins (2013). "Next-generation dynamic global vegetation models: Learning from community ecology". In: *New Phytologist* 198.3, pp. 957–969. DOI: 10.1111/nph.12210.

Sjöström, M., J. Ardö, A. Arneth, N. Boulain, B. Cappelaere, L. Eklundh, A. de Grandcourt, W. L. Kutsch, L. Merbold & Y. Nouvellon (2011). "Exploring the potential of MODIS EVI for modeling gross primary production across African ecosystems". In: *Remote Sensing of Environment* 115.4, pp. 1081–1089. DOI: 10.1016/j.rse.2010.12.013.

Smith, B. & J. B. Wilson (1996). "A consumer's guide to evenness indices". In: *Oikos* 76, pp. 70–82. DOI: 10.2307/3545749.

Stan, K. & A. Sanchez-Azofeifa (2019). "Tropical dry forest diversity, climatic response, and resilience in a changing climate". In: *Forests* 10.5, p. 443. DOI: 10.3390/f10050443.

Stöckli, R., T. Rutishauser, I. Baker, M. A. Liniger & A. S. Denning (2011). "A global reanalysis of vegetation phenology". In: *Journal of Geophysical Research* 116.G3. DOI: 10.1029/2010jg001545.

Velasque, M. & K. Del-Claro (2016). "Host plant phenology may determine the abundance of an ecosystem engineering herbivore in a tropical savanna". In: *Ecological Entomology* 41.4, pp. 421–430. DOI: 10.1111/een.12317.

White, M. A., K. M. de Beurs, K. Didan, D. W. Inouye, A. D. Richardson, O. P. Jensen, J. O'Keefe, G. Zhang, R. R. Nemani, W. J. D. Van Leeuwen, et al. (2009). "Intercomparison, interpretation, and assessment of spring phenology in North America estimated from remote sensing for 1982-

2006". In: *Global Change Biology* 15.10, pp. 2335–2359. DOI: 10.1111/j.1365-2486.2009.01910.x.

Whitecross, M. A., E. T. F. Witkowski & S. Archibald (2017). "Savanna tree-grass interactions: A phenological investigation of green-up in relation to water availability over three seasons". In: *South African Journal of Botany* 108, pp. 29–40. DOI: 10.1016/j.sajb.2016.09.003.

Whitley, R., J. Beringer, L. B. Hutley, G. Abramowitz, M. G. De Kauwe, B. Evans, V. Haverd, L. Li, C. Moore, Y. Ryu, et al. (2017). "Challenges and opportunities in land surface modelling of savanna ecosystems". In: *Biogeosciences* 14.20, pp. 4711–4732. DOI: 10.5194/bg-14-4711-2017.

Wilsey, B. J., D. R. Chalcraft, C. M. Bowles & M. R. Willig (2005). "Relationships among indices suggest that richness is an incomplete surrogate for grassland biodiversity". In: *Ecology* 86.5, pp. 1178–1184. DOI: 10.1890/04-0394.

Xia, J., S. Niu, P. Ciais, I. A. Janssens, J. Chen, C. Ammann, A. Arain, P. D. Blanken, A. Cescatti, D. Bonal, et al. (2015). "Joint control of terrestrial gross primary productivity by plant phenology and physiology". In: *Proceedings of the National Academy of Sciences* 112.9, pp. 2788–2793. DOI: 10.1073/pnas.1413090112.

Zani, D., T. W. Crowther, L. Mo, S. S. Renner & C. M. Zohner (2020). "Increased growing-season productivity drives earlier autumn leaf senescence in temperate trees". In: 370.6520, pp. 1066–1071. DOI: 10.1126/science.abd8911.

Zuur, A., E. N. Ieno, N. Walker, A. A. Saveliev & G. M. Smith (2009). *Mixed effects models and extensions in ecology with R*. New York NY, USA: Springer.

6 Supplementary Material

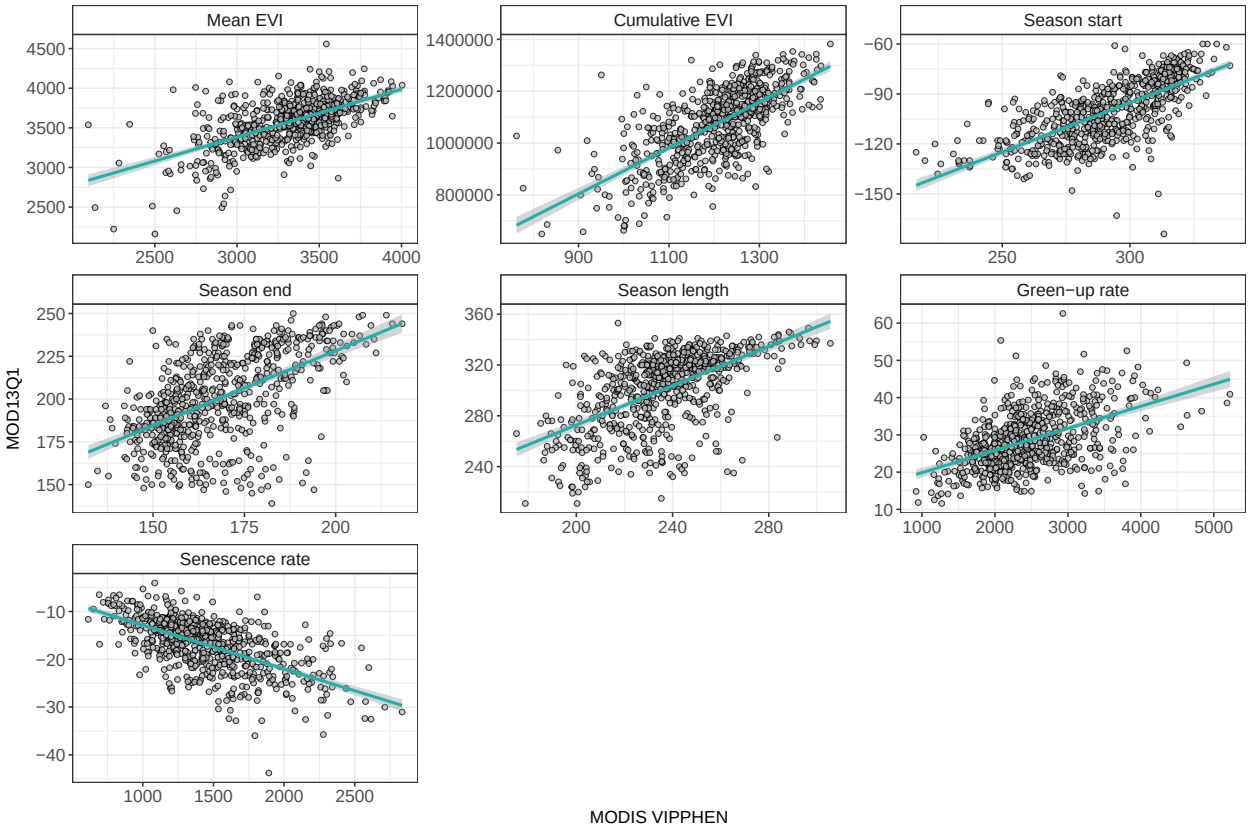

Figure S1: Scatter plots showing a comparison of phenological metrics from the MODIS VIPPHEN product (Didan & Barreto, 2016) and those extracted from the MOD13Q1 data (Didan, 2015), for each of the sites in our study. The cyan line shows a linear model of the data, with a 95% confidence interval.

Response	DoF	F	Prob.	R^2
Mean EVI	672	387.0	p<0.05	0.37
Cumulative EVI	672	592.6	p<0.05	0.47
Season start	672	660.3	p<0.05	0.50
Season end	672	285.0	p<0.05	0.30
Season length	672	325.0	p<0.05	0.33
Green-up rate	672	217.2	p<0.05	0.24
Senescence rate	672	412.3	p<0.05	0.38

Table S1: Model fit statistics for comparison of MODIS VIPPHEN and MOD13Q1 products across each of our study sites.

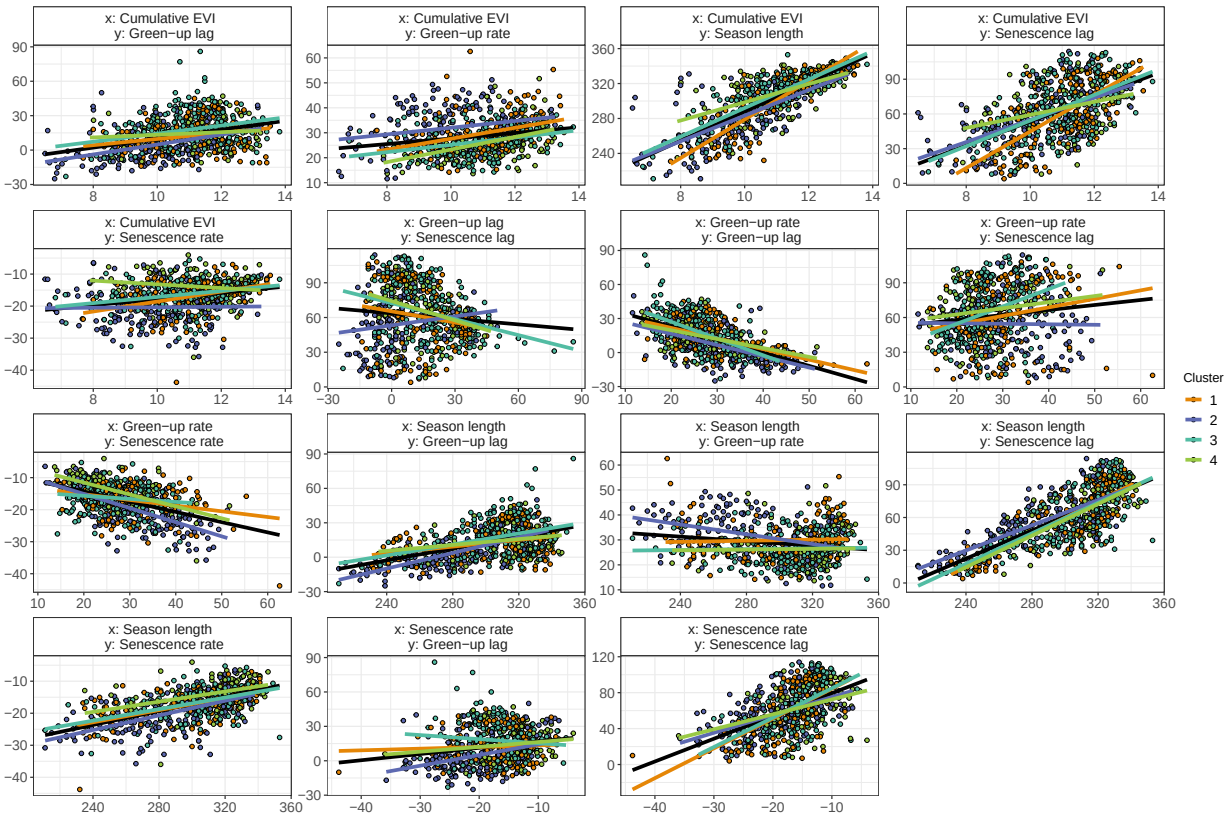

Figure S2: Scatter plots showing pairwise comparisons of the six phenological metrics used in this study, extracted from the MODIS MOD13Q1 product (Didan, 2015). Points represent study sites and are coloured by vegetation cluster. Linear regression line of best fit for all sites is shown as a black line, while linear regressions are shown for each vegetation cluster as coloured lines.

Rank	Precipitation	Diurnal dT	Evenness	Richness	Richness:Cluster	logLik	AIC	ΔIC	W_i
1	✓		✓	✓	**6**	**-1049**	**2110**	**0**	**0.461**
2	✓	✓	✓	✓	7	-1048	2110	1	0.355
3	✓			✓	5	-1052	2113	4	0.077
4	✓	✓		✓	6	-1051	2113	4	0.076
5	✓				4	-1055	2117	7	0.012
6	✓	✓			5	-1054	2118	8	0.010
7	✓		✓		5	-1055	2119	9	0.005
8	✓	✓	✓		6	-1054	2120	10	0.004
9		✓	✓	✓	6	-1115	2241	131	0.000
10			✓	✓	5	-1121	2252	142	0.000

Table S2: Cumulative EVI Model selection candidate models, with fit statistics. The overall best model is marked by bold text, according to AIC and model parsimony

Rank	Precipitation	Diurnal dT	Evenness	Richness	Richness:Cluster	logLik	AIC	ΔIC	W_i
1	✓	✓	✓	✓	7	-3178	6370	0	0.270
2	✓		✓	✓	**6**	**-3179**	**6370**	**0**	**0.264**
3	✓			✓	5	-3181	6372	2	0.104
4	✓				4	-3182	6372	2	0.102
5	✓	✓			5	-3181	6373	2	0.093
6	✓	✓		✓	6	-3180	6373	2	0.084
7	✓		✓		5	-3182	6374	4	0.042
8	✓	✓	✓		6	-3181	6374	4	0.042
9			✓	✓	5	-3194	6399	28	0.000
10		✓	✓	✓	6	-3194	6400	30	0.000

Table S3: Season length Model selection candidate models, with fit statistics. The overall best model is marked by bold text, according to AIC and model parsimony

Rank	Precipitation	Diurnal dT	Evenness	Richness	Richness:Cluster	logLik	AIC	ΔIC	W_i
1	✓	✓			**5**	**-2265**	**4540**	**0**	**0.478**
2	✓	✓	✓		6	-2265	4542	2	0.219
3	✓	✓		✓	6	-2265	4542	2	0.176
4	✓	✓	✓	✓	7	-2265	4544	3	0.094
5		✓			4	-2269	4547	7	0.018
6		✓	✓		5	-2269	4549	9	0.007
7		✓		✓	5	-2269	4549	9	0.007
8		✓	✓	✓	6	-2269	4551	11	0.002
9	✓				4	-2296	4601	60	0.000
10	✓			✓	5	-2296	4602	62	0.000

Table S4: Green-up rate Model selection candidate models, with fit statistics. The overall best model is marked by bold text, according to AIC and model parsimony

Rank	Precipitation	Diurnal dT	Evenness	Richness	Richness:Cluster	logLik	AIC	ΔIC	W_i
1	✓		✓	✓	6	-2048	4107	0	0.307
2	✓	✓	✓	✓	**7**	**-2047**	**4109**	**1**	**0.176**
3	✓				4	-2050	4109	1	0.159
4	✓		✓		5	-2050	4110	2	0.091
5	✓			✓	5	-2050	4110	2	0.089
6	✓	✓			5	-2050	4110	3	0.082
7	✓	✓	✓		6	-2049	4111	4	0.051
8	✓	✓		✓	6	-2050	4111	4	0.044
9		✓			4	-2058	4125	17	0.000
10		✓		✓	5	-2058	4126	18	0.000

Table S5: Senescence rate Model selection candidate models, with fit statistics. The overall best model is marked by bold text, according to AIC and model parsimony

Rank	Precipitation	Diurnal dT	Evenness	Richness	Richness:Cluster	logLik	AIC	ΔIC	W_i
1	✓	✓	✓	✓	**7**	**-2673**	**5361**	**0**	**1.000**
2	✓	✓		✓	6	-2683	5379	18	0.000
3	✓	✓	✓		6	-2684	5380	19	0.000
4	✓	✓			5	-2686	5381	20	0.000
5		✓	✓	✓	6	-2713	5439	78	0.000
6		✓	✓		5	-2732	5475	114	0.000
7		✓		✓	5	-2742	5494	133	0.000
8		✓			4	-2743	5494	133	0.000
9	✓		✓	✓	6	-2756	5523	162	0.000
10	✓			✓	5	-2760	5530	169	0.000

Table S6: Green-up lag Model selection candidate models, with fit statistics. The overall best model is marked by bold text, according to AIC and model parsimony

Rank	Precipitation	Diurnal dT	Evenness	Richness	Richness:Cluster	logLik	AIC	ΔIC	W_i
1	✓	✓			**5**	**-3105**	**6221**	**0**	**0.485**
2	✓	✓		✓	6	-3105	6222	2	0.215
3	✓	✓	✓		6	-3105	6223	2	0.192
4	✓	✓	✓	✓	7	-3105	6224	4	0.079
5		✓			4	-3110	6228	8	0.011
6		✓	✓		5	-3109	6229	8	0.009
7		✓		✓	5	-3110	6230	9	0.006
8		✓	✓	✓	6	-3109	6231	10	0.003
9					3	-3130	6266	45	0.000
10	✓				4	-3129	6267	46	0.000

Table S7: Senescence lag Model selection candidate models, with fit statistics. The overall best model is marked by bold text, according to AIC and model parsimony

Response	Clusters	Estimate	SE	DoF	T ratio	Prob.
Cumulative EVI	1-2	1.2E-16	2.93E-17	679	4.02	0.00
	1-3	3.1E-17	2.63E-17	678	1.17	0.65
	1-4	1.2E-17	3.64E-17	675	0.32	0.99
	2-3	-8.7E-17	2.63E-17	676	-3.30	0.01
	2-4	-1.1E-16	3.62E-17	674	-2.93	0.02
	3-4	-1.9E-17	3.38E-17	675	-0.57	0.94
Season length	1-2	1.9E-15	6.98E-16	680	2.69	0.04
	1-3	2.2E-16	6.30E-16	680	0.35	0.99
	1-4	-1.2E-15	8.67E-16	679	-1.37	0.52
	2-3	-1.7E-15	6.27E-16	676	-2.65	0.04
	2-4	-3.1E-15	8.63E-16	679	-3.56	0.00
	3-4	-1.4E-15	8.07E-16	679	-1.75	0.30
Green-up rate	1-2	-2.5E-16	1.80E-16	678	-1.38	0.51
	1-3	-1.0E-16	1.62E-16	679	-0.62	0.93
	1-4	9.3E-17	2.23E-16	679	0.42	0.98
	2-3	1.5E-16	1.64E-16	675	0.91	0.80
	2-4	3.4E-16	2.25E-16	678	1.52	0.43
	3-4	1.9E-16	2.10E-16	678	0.92	0.79
Senescence rate	1-2	3.0E-17	1.32E-16	677	0.22	1.00
	1-3	1.3E-17	1.19E-16	678	0.11	1.00
	1-4	-1.2E-16	1.63E-16	678	-0.72	0.89
	2-3	-1.6E-17	1.19E-16	674	-0.14	1.00
	2-4	-1.5E-16	1.63E-16	678	-0.90	0.80
	3-4	-1.3E-16	1.52E-16	678	-0.86	0.83
Green-up lag	1-2	8.7E-16	3.38E-16	680	2.59	0.05
	1-3	5.4E-16	3.04E-16	680	1.77	0.29
	1-4	4.8E-16	4.18E-16	679	1.15	0.66
	2-3	-3.4E-16	3.04E-16	676	-1.10	0.69
	2-4	-3.9E-16	4.17E-16	679	-0.94	0.78
	3-4	-5.7E-17	3.90E-16	679	-0.15	1.00
Senescence lag	1-2	1.3E-15	6.22E-16	674	2.10	0.16
	1-3	-1.7E-17	5.60E-16	663	-0.03	1.00
	1-4	-1.2E-15	7.75E-16	640	-1.61	0.38
	2-3	-1.3E-15	5.66E-16	677	-2.34	0.09
	2-4	-2.6E-15	7.78E-16	633	-3.28	0.01
	3-4	-1.2E-15	7.28E-16	638	-1.69	0.33

Table S8: Comparisons of interaction marginal effects using post-hoc Tukey's tests.

Response	Clusters	Mean diff.	Interval	Prob.
Cumulative EVI	2-1	-0.77	-1.05 - -0.5	p<0.01
	3-1	-0.09	-0.34 - 0.15	p = 0.76
	4-1	0.13	-0.18 - 0.44	p = 0.72
	3-2	0.68	0.43 - 0.93	p<0.01
	4-2	0.9	0.59 - 1.21	p<0.01
	4-3	0.22	-0.07 - 0.51	p = 0.20
Season length	2-1	-0.63	-0.9 - -0.36	p<0.01
	3-1	0.17	-0.07 - 0.42	p = 0.26
	4-1	0.32	0.01 - 0.63	p<0.05
	3-2	0.8	0.56 - 1.05	p<0.01
	4-2	0.95	0.64 - 1.26	p<0.01
	4-3	0.15	-0.14 - 0.43	p = 0.54
Green-up rate	2-1	0.27	-0.01 - 0.55	p = 0.06
	3-1	-0.43	-0.68 - -0.19	p<0.01
	4-1	-0.45	-0.77 - -0.14	p<0.01
	3-2	-0.7	-0.95 - -0.45	p<0.01
	4-2	-0.72	-1.04 - -0.41	p<0.01
	4-3	-0.02	-0.31 - 0.27	p = 1.00
Senescence rate	2-1	-0.62	-0.89 - -0.35	p<0.01
	3-1	0.12	-0.12 - 0.36	p = 0.58
	4-1	0.55	0.25 - 0.86	p<0.01
	3-2	0.74	0.49 - 0.98	p<0.01
	4-2	1.17	0.86 - 1.48	p<0.01
	4-3	0.43	0.15 - 0.72	p<0.01
Green-up lag	2-1	-0.49	-0.77 - -0.21	p<0.01
	3-1	0.32	0.07 - 0.57	p<0.01
	4-1	0.14	-0.18 - 0.45	p = 0.67
	3-2	0.81	0.56 - 1.06	p<0.01
	4-2	0.63	0.31 - 0.94	p<0.01
	4-3	-0.18	-0.47 - 0.11	p = 0.38
Senescence lag	2-1	-0.25	-0.54 - 0.03	p = 0.10
	3-1	0.13	-0.13 - 0.39	p = 0.57
	4-1	0.2	-0.13 - 0.52	p = 0.41
	3-2	0.38	0.13 - 0.64	p<0.01
	4-2	0.45	0.12 - 0.78	p<0.01
	4-3	0.07	-0.23 - 0.37	p = 0.94

Table S9: Post-hoc Tukey's pairwise comparisons among vegetation types for each phenological metric.